

A Scotogenic Model with Two Inert Doublets

Amine Ahriche 

Department of Applied Physics and Astronomy, University of Sharjah, P.O. Box 27272 Sharjah, UAE.

E-mail: ahriche@sharjah.ac.ae

ABSTRACT: In this work, we present a scotogenic model, where the neutrino mass is generated at one-loop diagrams. The standard model (SM) is extended by three singlet Majorana fermions and two inert scalar doublets instead of one doublet as in the minimal scotogenic model. The model scalar sector includes two CP-even, two CP-odd and two charged scalars in addition to the Higgs. The dark matter (DM) candidate could be either the light Majorana fermion (Majorana DM), or the lightest among the CP-even and the CP-odd scalars (scalar DM). We show that the model accommodates both Majorana and scalar DM within a significant viable parameter space, while considering all the relevant theoretical and experimental constraints such as perturbativity, vacuum stability, unitarity, the di-photon Higgs decay, electroweak precision tests and lepton flavor violating constraints. In addition to the collider signatures predicted by the minimal scotogenic model, our model predicts some novel signatures that can be probed through some final states such as $8 \text{ jets} + \cancel{E}_T$, $1\ell + 4 \text{ jets} + \cancel{E}_T$ and $4b + \cancel{E}_T$.

Contents

1	Introduction	1
2	The Model & Neutrino Mass	3
3	Theoretical & Experimental Constraints	6
4	Viable Parameter Space	9
5	Dark Matter: Majorana or Scalar?	12
6	Conclusion	15
A	Generalized Casas-Ibarra parameterization	16
B	Scotogenic Model with n inert Doublets	17
C	The Unitarity Amplitude Matrices	18

1 Introduction

The standard model (SM) of particle physics was successful in describing the properties of elementary particles and their interactions around the electroweak (EW) scale. However, there are still unanswered questions such as the neutrino oscillation data and the dark matter (DM) nature. Neutrino oscillation data established that at least two of the three SM neutrinos have mass and nonzero mixing. However, their properties, such as their nature and the origin of the smallness of their mass, have no explanation within the SM, which demands for new physics. One of the most popular mechanisms to explain why neutrino mass is tiny; is the so-called seesaw mechanism [1], which assumes the existence of right-handed (RH) neutrinos with masses that are heavier by several orders of magnitude than the EW scale. Such heavy particles decouple from the low-energy spectrum at the EW scale, and hence, cannot be directly probed at high-energy physics experiments. Another approach that requires lower new physics scale, where small neutrino mass is generated naturally; is via quantum corrections, where loop suppression factor(s) ensures the neutrino mass smallness. This can be realized at one loop [2], two loops [3], three loops [4, 5], or four loops [6]. Interesting features for this TeV scale new physics class of models can be tested at high energy colliders [7, 8] (For a review, see [9]).

The simplest and most popular realization of a radiative neutrino mass mechanism is the so-called scotogenic model [10], where the SM is extended by an inert scalar doublet and three singlet Majorana fermions. In addition, this model could accommodate two possible DM candidates, i.e., the lightest among the Majorana fermions and the light neutral scalar in the inert dark doublet. The scalar DM scenario is identical to the inert doublet Higgs model (IDM), that is highly constrained by the DM direct detection experiments. In the scenario of Majorana DM, the right amount of the DM relic density requires relatively large values for the new Yukawa couplings that couple the inert doublet with the Majorana fermions [11, 12]. This can be achieved only by imposing a strong degeneracy between the masses of the CP-even and CP-odd scalars, making the quartic coupling suppressed $\lambda_5 \sim 10^{-10} - 10^{-9}$. Such fine-tuning can be avoided by extending the minimal scotogenic model (MSctM) by two real singlets and impose a global Z_4/Z_2 symmetry [13]. Indeed, there have many models that have been proposed and studied beyond the MSctM [14, 15]. For example, in [14] the authors studied a generalized scotogenic model, or what they called "*general scotogenic model*", by considering n_N Majorana singlet fermions and n_η inert doublets, where many phenomenological aspects were discussed.

Based on the current/future results of both ATLAS and CMS, the IDM (and therefore, the MSctM with scalar DM model) parameter space will become more constrained as the precision measurements of the EW sector gets improved. In addition, the recent results from the direct detection experiments such as LUX-ZEPLIN experiment [16], would place more stringent bounds on the model. This makes the extension of the IDM interesting, that might evade some of the constraints and predict additional interesting signatures. On top of that, among the important motivations to extend the IDM; is that it does not allow CP violation in the scalar sector, where an additional $SU(2)_L$ Higgs doublet is useful to do this task [17]. According to the previously mentioned motivations, it is natural to consider the realization of a scotogenic model where the SM is extended by three singlet Majorana fermions $N_{1,2,3}$ and two inert doublets $\Phi_{1,2}$ that couple to the leptonic left-handed doublets and the singlet Majorana's. Here, the new additional fields transform as odd fields under a global Z_2 symmetry $\{N_{1,2,3}, \Phi_{1,2}\} \rightarrow \{-N_{1,2,3}, -\Phi_{1,2}\}$ to ensure the DM stability.

This work is organized as follow. In section 2, we present the model and show the neutrino mass generation at loop. In section 3, different theoretical and experimental constraints are discussed. Sections 4 and 5 are devoted to show the viable parameter space and the DM phenomenology, respectively, in both scenarios of Majorana and scalar DM candidates. We conclude in section 6. In addition, the paper includes three appendices: in Appendix A, we discuss how to estimate the new Yukawa couplings where a generalized parameterization like the Casas-Ibarra one is introduced. In Appendix B, we generalize

our results for the case of a scotogenic model with \mathbf{n} inert scalar doublets instead of two. In Appendix C, we give the amplitude matrices that are relevant to the perturbative unitarity conditions.

2 The Model & Neutrino Mass

Here, we extend the SM by two inert doublets denoted by $\Phi_{1,2} \sim (1, 2, 1)$ and three singlet Majorana fermions $N_i \sim (1, 1, 0)$. The Lagrangian that involves the Majorana fermions can be written as

$$\mathcal{L} \supset \bar{L}_\alpha (h_{\alpha,k} \epsilon \cdot \Phi_1 + h_{\alpha,k+3} \epsilon \cdot \Phi_2) N_k + \frac{1}{2} \bar{N}_k^c M_k N_k + h.c., \quad (2.1)$$

where L_α are the left-handed lepton doublets, and $\epsilon = i\sigma_2$ is an anti-symmetric tensor. Here, $h_{\alpha,k}$ is a 3×6 new Yukawa matrix, the mass matrix M_k can be considered diagonal.

The most general Z_2 -symmetric, renormalizable, and gauge invariant potential reads

$$\begin{aligned} V(\mathcal{H}, \Phi, S, \chi) = & -\mu_H^2 |\mathcal{H}|^2 + \mu_i^2 |\Phi_i|^2 + \frac{\lambda_H}{6} |\mathcal{H}|^4 + \frac{\lambda_i}{6} |\Phi_i|^4 + \omega_i |\mathcal{H}|^2 |\Phi_i|^2 + \kappa_i |\mathcal{H}^\dagger \Phi_i|^2 \\ & + \varrho_1 |\Phi_1|^2 |\Phi_2|^2 + \varrho_2 |\Phi_1^\dagger \Phi_2|^2 + \left\{ \mu_3^2 \Phi_1^\dagger \Phi_2 + \frac{1}{2} \zeta_i (\mathcal{H}^\dagger \Phi_i)^2 + \zeta_3 (\mathcal{H}^\dagger \Phi_1) (\mathcal{H}^\dagger \Phi_2) \right. \\ & \left. + \zeta_4 (\Phi_1^\dagger \mathcal{H}) (\mathcal{H}^\dagger \Phi_2) + h.c. \right\}, \end{aligned} \quad (2.2)$$

with \mathcal{H} , and Φ can be parameterized as follows

$$\mathcal{H} = \begin{pmatrix} \chi^+ \\ \frac{1}{\sqrt{2}}(v + h + i\chi^0) \end{pmatrix}, \quad \Phi_i = \begin{pmatrix} S_i^+ \\ \frac{1}{\sqrt{2}}(S_i^0 + iQ_i^0) \end{pmatrix}. \quad (2.3)$$

The terms of the Lagrangian in (2.1) and (2.2) are invariant under a global Z_2 symmetry according to the charges

$$\Phi_{1,2} \rightarrow -\Phi_{1,2}, \quad N_{1,2,3} \rightarrow -N_{1,2,3}, \quad (2.4)$$

where all other fields are even. This Z_2 symmetry forbids such terms like $(\mathcal{H}^\dagger \Phi_i) (\Phi_j^\dagger \Phi_k)$. In case of complex values for μ_3^2 and/or ζ_i , CP is explicitly broken, where we obtain CP-violating interactions relevant to the four neutral inert eigenstates in the basis $\{S_1^0, S_2^0, Q_1^0, Q_2^0\}$. This case would be very interesting since the additional CP-violating sources are required for matter antimatter asymmetry generation [18]. In what follows, we consider real values for the parameters μ_3^2 and $\zeta_{i=1,2,3,4}$ to avoid CP violation. The case of explicit CP violation (complex values for μ_3^2 and/or ζ_i) requires an independent investigation since it may have important cosmological consequences.

After the electroweak symmetry breaking (EWSB), we are left with three CP-even scalars $(h, H_{1,2}^0)$, two CP-odd scalar $A_{1,2}^0$ and two pair of charged scalars $H_{1,2}^\pm$. The Higgs

mass is given $m_h^2 = 2\mu_H^2 = \frac{\lambda_H}{3}v^2$, and the inert eigenstates are defined as

$$\begin{aligned} \begin{pmatrix} H_1^0 \\ H_2^0 \end{pmatrix} &= \begin{pmatrix} c_H & s_H \\ -s_H & c_H \end{pmatrix} \begin{pmatrix} S_1^0 \\ S_2^0 \end{pmatrix}, \quad \begin{pmatrix} A_1^0 \\ A_2^0 \end{pmatrix} = \begin{pmatrix} c_A & s_A \\ -s_A & c_A \end{pmatrix} \begin{pmatrix} Q_1^0 \\ Q_2^0 \end{pmatrix}, \\ \begin{pmatrix} H_1^\pm \\ H_2^\pm \end{pmatrix} &= \begin{pmatrix} c_C & s_C \\ -s_C & c_C \end{pmatrix} \begin{pmatrix} S_1^\pm \\ S_2^\pm \end{pmatrix}, \end{aligned} \quad (2.5)$$

with $c_X = \cos \theta_X$, $s_X = \sin \theta_X$ and θ_H , θ_A and θ_C are the mixing angles that diagonalise the CP -even, CP -odd and charged scalars mass matrices, respectively. The charged, neutral CP -even and CP -odd scalar squared mass matrices in the basis $\{S_1^\pm, S_2^\pm\}$, $\{S_1^0, S_2^0\}$ and $\{Q_1^0, Q_2^0\}$, respectively, are given by

$$M_C^2 = \begin{bmatrix} \mu_1^2 & \mu_3^2 \\ \mu_3^2 & \mu_2^2 \end{bmatrix} + \frac{v^2}{2} \begin{bmatrix} \omega_1 & 0 \\ 0 & \omega_2 \end{bmatrix}, \quad M_{H,A}^2 = M_C^2 + \frac{v^2}{2} \begin{bmatrix} \kappa_1 & \zeta_4 \\ \zeta_4 & \kappa_2 \end{bmatrix} \pm \frac{v^2}{2} \begin{bmatrix} \xi_1 & \xi_3 \\ \xi_3 & \xi_2 \end{bmatrix}. \quad (2.6)$$

The mass eigenvalues and the mixing are given by

$$\begin{aligned} m_{X_{1,2}}^2 &= \frac{1}{2} \left([M_X^2]_{11} + [M_X^2]_{22} \mp \sqrt{([M_X^2]_{22} - [M_X^2]_{11})^2 + 4[M_X^2]_{12}^2} \right), \\ \tan(2\theta_X) &= 2[M_X^2]_{12} / ([M_X^2]_{22} - [M_X^2]_{11}), \end{aligned} \quad (2.7)$$

for $([X_{1,2}, \theta_X] = [H_{1,2}^0, \theta_H], [A_{1,2}^0, \theta_A], [H_{1,2}^\pm, \theta_C])$, respectively.

Then, the independent free parameters are

$$M_{1,2,3}, m_{H_{1,2}^\pm}, m_{H_{1,2}^0}, m_{A_{1,2}^0}, s_{H,A,C}, \omega_{1,2}, h_{\alpha i}, \quad (2.8)$$

where

$$\begin{aligned} \mu_1^2 &= m_{H_1^\pm}^2 c_C^2 + m_{H_2^\pm}^2 s_C^2 - \frac{1}{2} \omega_1 v^2, \quad \mu_2^2 = m_{H_1^\pm}^2 s_C^2 + m_{H_2^\pm}^2 c_C^2 - \frac{1}{2} \omega_2 v^2, \quad \mu_3^2 = c_C s_C (m_{H_2^\pm}^2 - m_{H_1^\pm}^2), \\ \kappa_1 v^2 &= m_{H_1^0}^2 c_H^2 + m_{H_2^0}^2 s_H^2 + m_{A_1^0}^2 c_A^2 + m_{A_2^0}^2 s_A^2 - 2(m_{H_1^\pm}^2 c_C^2 + m_{H_2^\pm}^2 s_C^2), \\ \kappa_2 v^2 &= m_{H_2^0}^2 c_H^2 + m_{H_1^0}^2 s_H^2 + m_{A_2^0}^2 c_A^2 + m_{A_1^0}^2 s_A^2 - 2(m_{H_2^\pm}^2 c_C^2 + m_{H_1^\pm}^2 s_C^2), \\ \xi_1 v^2 &= (m_{H_1^0}^2 c_H^2 + m_{H_2^0}^2 s_H^2) - (m_{A_2^0}^2 s_A^2 + m_{A_1^0}^2 c_A^2), \quad \xi_2 v^2 = (m_{H_1^0}^2 s_H^2 + m_{H_2^0}^2 c_H^2) - (m_{A_1^0}^2 s_A^2 + m_{A_2^0}^2 c_A^2), \\ \xi_3 v^2 &= s_H c_H (m_{H_2^0}^2 - m_{H_1^0}^2) - s_A c_A (m_{A_2^0}^2 - m_{A_1^0}^2), \\ \xi_4 v^2 &= s_H c_H (m_{H_2^0}^2 - m_{H_1^0}^2) + s_A c_A (m_{A_2^0}^2 - m_{A_1^0}^2) - 2c_C s_C (m_{H_2^\pm}^2 - m_{H_1^\pm}^2). \end{aligned} \quad (2.9)$$

The first term in (2.1), can be written as

$$\mathcal{L} \supset \sum_{\alpha,j,k} \frac{1}{\sqrt{2}} (g_{\alpha k}^{(j)} H_j^0 + i f_{\alpha k}^{(j)} A_j^0) \bar{\nu}_{\alpha L} N_k - \zeta_{\alpha k}^{(j)} H_j^\pm \bar{\ell}_{\alpha L} N_k + h.c., \quad (2.10)$$

with $\alpha = e, \mu, \tau, j = 1, 2$ and $k = 1, 3$; and

$$\begin{aligned} g_{\alpha k}^{(1)} &= c_H h_{\alpha, k} + s_H h_{\alpha, k+3}, & g_{\alpha k}^{(2)} &= -s_H h_{\alpha, k} + c_H h_{\alpha, k+3}, \\ f_{\alpha k}^{(1)} &= c_A h_{\alpha, k} + s_A h_{\alpha, k+3}, & f_{\alpha k}^{(2)} &= -s_A h_{\alpha, k} + c_A h_{\alpha, k+3}, \\ \zeta_{\alpha k}^{(1)} &= c_C h_{\alpha, k} + s_C h_{\alpha, k+3}, & \zeta_{\alpha k}^{(2)} &= -s_C h_{\alpha, k} + c_C h_{\alpha, k+3}. \end{aligned} \quad (2.11)$$

The first two interaction terms in (2.10) give rise to the neutrino mass a la scotogenic way; and the last term leads to the LFV processes $\ell_\beta \rightarrow \ell_\alpha + \gamma$ and $\ell_\beta \rightarrow 3\ell_\alpha$. Then, the neutrino mass $[\alpha, \beta]$ matrix element comes from the contribution 12 diagrams as shown in Fig. 1.

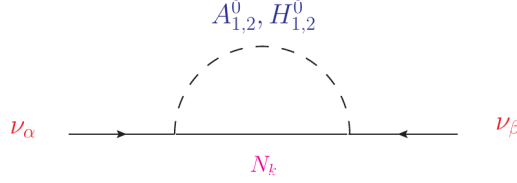


Figure 1: The 12 Feynman diagrams responsible for neutrino mass generation.

It can be written as

$$m_{\alpha\beta}^{(\nu)} = \sum_{k=1}^3 \sum_{j=1}^2 M_k \left\{ g_{\alpha k}^{(j)} g_{\beta k}^{(j)} \mathcal{F}\left(m_{H_j^0}/M_k\right) - f_{\alpha k}^{(j)} f_{\beta k}^{(j)} \mathcal{F}\left(m_{A_j^0}/M_k\right) \right\}, \quad (2.12)$$

with $\mathcal{F}(x) = \frac{x^2 \log(x)}{8\pi^2(x^2-1)}$. The divergent parts of the diagrams in Fig. 1 that are mediated by H_j^0 and A_j^0 cancels each other due to the identity¹

$$\sum_{j=1}^2 \left\{ g_{\alpha k}^{(j)} g_{\beta k}^{(j)} - f_{\alpha k}^{(j)} f_{\beta k}^{(j)} \right\} = 0. \quad (2.13)$$

The neutrino mass matrix (2.12) can be parameterized as

$$(m^{(\nu)})_{3 \times 3} = (h)_{3 \times 6} \cdot (\Lambda)_{6 \times 6} \cdot (h^T)_{6 \times 3}, \quad (2.14)$$

$$\Lambda = \begin{pmatrix} \omega_1 & \omega_3 \\ \omega_3 & \omega_2 \end{pmatrix}, \quad (2.15)$$

where $\omega_{1,2,3}$ are 3×3 diagonal matrices whose elements are given by

$$\begin{aligned} (\omega_1)_{ik} &= \delta_{ik} M_k \left[c_H^2 \mathcal{F}\left(m_{H_1^0}/M_k\right) + s_H^2 \mathcal{F}\left(m_{H_2^0}/M_k\right) - c_A^2 \mathcal{F}\left(m_{A_1^0}/M_k\right) - s_A^2 \mathcal{F}\left(m_{A_2^0}/M_k\right) \right], \\ (\omega_2)_{ik} &= \delta_{ik} M_k \left[s_H^2 \mathcal{F}\left(m_{H_1^0}/M_k\right) + c_H^2 \mathcal{F}\left(m_{H_2^0}/M_k\right) - s_A^2 \mathcal{F}\left(m_{A_1^0}/M_k\right) - c_A^2 \mathcal{F}\left(m_{A_2^0}/M_k\right) \right], \\ (\omega_3)_{ik} &= \delta_{ik} M_k \left[s_H c_H \left(\mathcal{F}\left(m_{H_1^0}/M_k\right) - \mathcal{F}\left(m_{H_2^0}/M_k\right) \right) - s_A c_A \left(\mathcal{F}\left(m_{A_1^0}/M_k\right) - \mathcal{F}\left(m_{A_2^0}/M_k\right) \right) \right], \end{aligned} \quad (2.16)$$

¹One has to mention that this identity is equivalent to (18) in [14], where the scotogenic model is generalized by considering many Majorana singlets and inert doublets.

for $i, k = 1, 3$. Here, the matrix Λ in (2.14) is not diagonal, and therefore cannot use the Casas-Ibarra parameterization [19] to estimate the Yukawa couplings h . However, we can derive a similar formula in such case (Λ is not diagonal). We give a general solution for the Yukawa coupling $3 \times M$ matrix² as

$$h_{3 \times M} = (U_\nu)_{3 \times 3} \cdot (D_{\sqrt{m_\nu}})_{3 \times 3} \cdot (T)_{3 \times M} \cdot (D_{(\Lambda'_i)^{-1/2}})_{M \times M} \cdot (Q)_{M \times M} \quad , \quad (2.17)$$

with U_ν is the Pontecorvo-Maki-Nakawaga-Sakata (PMNS) mixing matrix, $D_{\sqrt{m_\nu}} = \text{diag}\{m_1^{1/2}, m_2^{1/2}, m_3^{1/2}\}$ with m_i are the neutrino mass eigenvalues; and T is an arbitrary $3 \times M$ matrix that fulfills the identity $T_{3 \times M} \cdot T_{M \times 3}^T = \mathbf{1}_{3 \times 3}$. The matrix $(D_{(\Lambda'_i)^{-1/2}})_{M \times M} = \text{diag}\{(\Lambda'_i)^{-1/2}\}$, with Λ'_i to be the eigenvalues of the matrix Λ in (2.14), that diagonalized using the matrix Q , i.e., $\text{diag}\{\Lambda'_i\} = Q \cdot \Lambda \cdot Q^T$. In Appendix A, we discuss the derivation of (2.17) and the possible representations for this matrix. In addition, we discuss in Appendix B the generalization of this model by considering \mathbf{n} inert scalar doublets instead of two doublets.

3 Theoretical & Experimental Constraints

Here, we discuss the theoretical and the experimental constraints relevant to our model. These constraints are briefly discussed below:

- **Perturbativity:** all the quartic vertices of the scalar fields should be satisfy the perturbativity bounds, i.e.,

$$\max \left\{ \lambda_H, \lambda_{1,2}, |\omega_{1,2}|, |\kappa_{1,2} + \omega_{1,2}|, |\omega_{1,2} + \kappa_{1,2} \pm \xi_{1,2}|, |\varrho_1|, |\varrho_1 + \varrho_2|, |\xi_{1,2}|, \frac{1}{2}|\kappa_{1,2} \pm \xi_{1,2}|, \frac{1}{2}|\varrho_2| \right\} \leq 4\pi. \quad (3.1)$$

- **Perturbative unitarity:** the perturbative unitarity has to be preserved in all processes involving scalars or gauge bosons. In the high-energy limit, the gauge bosons should be replaced by their Goldstones; and the scattering amplitude matrix of $\phi_i \phi_j \rightarrow \phi_k \phi_m$ can be easily calculated. It has been shown that the perturbative unitarity conditions are achieved if the eigenvalues of the scattering amplitude matrix to be smaller than $|\Lambda_i| < 8\pi$ [20].

In our model, due to some exact symmetries such as the electric charge, CP and the global Z_2 symmetry, the full scattering amplitude matrix can be divided into six sub-matrices. These six sub-matrices are defined in the basis of initial/final states that are: (1) CP-even, Z_2 even, & $Q_{em} = 0$; (2) CP-even, Z_2 odd, & $Q_{em} = 0$, (3) CP-odd, Z_2 even, & $Q_{em} = 0$, (4) CP-odd, Z_2 odd, & $Q_{em} = 0$, (5) Z_2 even, & $Q_{em} = \pm 1$; and (6) Z_2 odd, & $Q_{em} = \pm 1$. These sub-matrices and their basis are given in Appendix C in details.

²Here, $M = 6$ in our case. However, the solutions (2.17) are valid for any value $M \geq 3$.

- **Vacuum Stability:** the scalar potential is required to be bounded from below in all the directions of the field space. It is obvious that along the pure directions ($\Phi_1 = \Phi_2 = 0$), ($\mathcal{H} = \Phi_2 = 0$) and ($\mathcal{H} = \Phi_1 = 0$), the vacuum stability conditions, i.e., the potential positivity at large field values, are $\lambda_H, \lambda_1, \lambda_2 > 0$, respectively. However, along any direction beside the pure ones, the potential positivity is guaranteed if all quartic couplings are positive. In case of negative quartic coupling(s), the vacuum stability conditions are [21]:

$$\left| \begin{array}{ccc} \lambda_H & \overline{\omega_1 + \kappa_1 + \xi_1} & \overline{\omega_2 + \kappa_2 + \xi_2} \\ \frac{\overline{\omega_1 + \kappa_1 + \xi_1}}{\overline{\omega_2 + \kappa_2 + \xi_2}} & \lambda_1 & \frac{\overline{\omega_2 + \kappa_2 + \xi_2}}{\varrho_1 + \varrho_2} \\ \frac{\overline{\omega_2 + \kappa_2 + \xi_2}}{\varrho_1 + \varrho_2} & \frac{\overline{\omega_1 + \kappa_1 + \xi_1}}{\varrho_1 + \varrho_2} & \lambda_2 \end{array} \right| > 0, \quad \left| \begin{array}{ccc} \frac{2}{3}\lambda_H & \overline{\omega_1 + \kappa_1} & \overline{\omega_2 + \kappa_2} \\ \frac{\overline{\omega_1 + \kappa_1}}{\overline{\omega_2 + \kappa_2}} & \frac{2}{3}\lambda_1 & \frac{\overline{\omega_2 + \kappa_2}}{\varrho_1 + \varrho_2} \\ \frac{\overline{\omega_2 + \kappa_2}}{\varrho_1 + \varrho_2} & \frac{\overline{\omega_1 + \kappa_1}}{\varrho_1 + \varrho_2} & \frac{2}{3}\lambda_2 \end{array} \right| > 0, \quad (3.2)$$

for the neutral and charged fields directions, respectively, with $\overline{X} = \min(X, 0)$.

In addition, we require that the vacuum ($\langle h \rangle = v, \langle S_i^0 \rangle = 0$) would be the deepest one. As a conservative choice in this work, we consider the conditions that the potential (2.2) should not develop a vev in the inert directions, i.e., we should have $\langle S_i^0 \rangle = 0$ either at $\langle h \rangle = 0$ or $\langle h \rangle = v$. These conditions can be translated into

$$\mu_1^2, \mu_2^2, \mu_1^2 + \mu_2^2 - \sqrt{(\mu_2^2 - \mu_1^2)^2 + 4(\mu_3^2)^2} > 0, \quad (3.3)$$

and obviously, $m_{H_1^0}^2, m_{A_1^0}^2, m_{H_1^\pm}^2 > 0$.

- **Gauge bosons decay widths:** The decay widths of the W/Z -bosons were measured with high precision at LEP. Therefore, we require that the decays of W/Z -bosons to Z_2 -odd scalars is closed. This is fulfilled if one assumes that

$$\min(m_{H_1^0} + m_{A_1^0}, 2m_{H_1^\pm}) > m_Z, \quad \min(m_{H_1^\pm} + m_{A_1^0}, m_{H_1^\pm} + m_{H_1^0}) > m_W. \quad (3.4)$$

- **Lepton flavor violating (LFV) decays:** in this model, LFV decay processes arise via one-loop diagrams mediated by the $H_{i=1,2}^\pm$ and N_k particles. The branching ratio of the decay $\mathcal{B}(\ell_\alpha \rightarrow \ell_\beta + \gamma)$ due to the contribution of the interactions (2.1) is [22]:

$$\mathcal{B}(\ell_\alpha \rightarrow \ell_\beta + \gamma) = \frac{3\alpha v^4}{32\pi} \left| \sum_{k=1}^3 \sum_{j=1}^2 \frac{(\zeta_{\alpha k}^{(j)})(\zeta_{\beta k}^{(j)})^*}{m_{H_j^\pm}^2} F\left(\frac{M_k^2}{m_{H_j^\pm}^2}\right) \right|^2, \quad (3.5)$$

where $\alpha = e^2/4\pi$ is the electromagnetic fine structure constant and $F(x) = (1 - 6x + 3x^2 + 2x^3 - 6x^2 \log x)/6(1-x)^4$. Since the bounds on $\ell_\alpha \rightarrow \ell_\beta + \gamma$ are more severe, especially $\mu \rightarrow e + \gamma$, we will consider only the LFV bounds on $\ell_\alpha \rightarrow \ell_\beta + \gamma$ and not $\ell_\alpha \rightarrow \ell_\beta \ell_\beta \ell_\beta$, since the latter's would implicitly fulfilled [23].

One has to notice that getting experimentally allowed values for the branching ratios (3.5) can be achieved by considering very small Yukawa couplings $h_{\alpha i}$ and/or very

heavy charged scalars. Although, this choice is preferred by the scalar DM case, but not interesting from Majorana DM relic density and/or collider point of view. However, one can consider well chosen values for the Yukawa couplings ($h_{\alpha i}$) and the Majorana and charged scalar masses, where the terms in the summation in (3.5) cancel each other. This allows relatively large Yukawa couplings as well relatively light charged scalars in order to accommodate the DM relic density in the case of Majorana DM [11, 13]; and provide interesting predictions at colliders [8, 11, 12, 23]. This can be clearly seen when comparing the Yukawa couplings and the Majorana and scalar masses for the two benchmark points (BPs) in Table 1 that corresponds to Majorana and scalar DM cases.

- **Direct searches of charginos and neutralinos at the LEP-II experiment:** we use the null results of neutralinos and charginos at LEP [24] to put lower bounds on the masses of charged Higgs H_1^\pm and the light neutral scalars of the inert doublets (H_1^0, A_1^0). The bound obtained from a re-interpretation of neutralino searches [25] cannot apply to our model since the decays $A_1^0 \rightarrow H_1^\pm Z (\rightarrow \ell^+ \ell^-)$ are kinematically forbidden. On the other hand, in most regions of the parameter space, the charged Higgs decays exclusively into a Majorana fermion and a charged lepton. For Yukawa couplings of order one $h_{ei} \simeq \mathcal{O}(1)$, the following bounds are derived $m_{H^\pm} > 100$ GeV [12].
- **The electroweak precision tests:** in this model, the oblique parameters acquire contributions from the existence of inert scalars. We take $\Delta U = 0$ in our analysis, the oblique parameters are given by [26]

$$\begin{aligned}
\Delta T &= \frac{1}{16\pi s_w^2 M_W^2} \left\{ c_H^2 c_C^2 F(m_{H_1^0}^2, m_{H_1^\pm}^2) + c_H^2 s_C^2 F(m_{H_1^0}^2, m_{H_2^\pm}^2) + s_H^2 c_C^2 F(m_{H_2^0}^2, m_{H_1^\pm}^2) \right. \\
&\quad + s_H^2 s_C^2 F(m_{H_2^0}^2, m_{H_2^\pm}^2) + c_A^2 c_C^2 F(m_{A_1^0}^2, m_{H_1^\pm}^2) + c_A^2 s_C^2 F(m_{A_1^0}^2, m_{H_2^\pm}^2) + s_A^2 c_C^2 F(m_{A_1^0}^2, m_{H_1^\pm}^2) \\
&\quad + s_A^2 s_C^2 F(m_{A_1^0}^2, m_{H_2^\pm}^2) - c_H^2 c_A^2 F(m_{H_1^0}^2, m_{A_1^0}^2) - c_H^2 s_A^2 F(m_{H_1^0}^2, m_{A_2^0}^2) - s_H^2 c_A^2 F(m_{H_2^0}^2, m_{A_1^0}^2) \\
&\quad \left. - s_H^2 s_A^2 F(m_{H_2^0}^2, m_{A_2^0}^2) \right\}, \\
\Delta S &= \frac{1}{24\pi} \left\{ (2s_w^2 - 1)^2 \left[c_C^4 G(m_{H_1^\pm}^2, m_{H_1^\pm}^2, m_Z^2) + s_C^4 G(m_{H_2^\pm}^2, m_{H_2^\pm}^2, m_Z^2) + 2c_C^2 s_C^2 G(m_{H_1^\pm}^2, m_{H_2^\pm}^2, m_Z^2) \right] \right. \\
&\quad + c_H^2 c_A^2 G(m_{H_1^0}^2, m_{A_1^0}^2, m_Z^2) + c_H^2 s_A^2 G(m_{H_1^0}^2, m_{A_2^0}^2, m_Z^2) + s_H^2 c_A^2 G(m_{H_2^0}^2, m_{A_1^0}^2, m_Z^2) \\
&\quad + s_H^2 s_A^2 G(m_{H_2^0}^2, m_{A_2^0}^2, m_Z^2) + c_H^2 c_C^2 \log\left(\frac{m_{H_1^0}^2}{m_{H_1^\pm}^2}\right) + c_H^2 s_C^2 \log\left(\frac{m_{H_1^0}^2}{m_{H_2^\pm}^2}\right) + s_H^2 c_C^2 \log\left(\frac{m_{H_2^0}^2}{m_{H_1^\pm}^2}\right) \\
&\quad + s_H^2 s_C^2 \log\left(\frac{m_{H_2^0}^2}{m_{H_2^\pm}^2}\right) + c_H^2 c_A^2 \log\left(\frac{m_{A_1^0}^2}{m_{H_1^\pm}^2}\right) + c_H^2 s_A^2 \log\left(\frac{m_{A_2^0}^2}{m_{H_1^\pm}^2}\right) + s_H^2 c_A^2 \log\left(\frac{m_{A_1^0}^2}{m_{H_2^\pm}^2}\right) \\
&\quad \left. + s_H^2 s_A^2 \log\left(\frac{m_{A_2^0}^2}{m_{H_2^\pm}^2}\right) \right\}, \tag{3.6}
\end{aligned}$$

where $s_W \equiv \sin \theta_W$, with θ_W is the Weinberg mixing angle, and $F(x, y)$ and $G(x, y, z)$ are one-loop functions that can be found in [26].

- **The di-photon Higgs decay:** the Higgs couplings to the two charged scalar can change drastically the value of the Higgs boson loop-induced decay into two photons. These loop interactions depends on the signs and the values of $\omega_{1,2}$, as well on the mixing and θ_C . The ratio $R_{\gamma\gamma} = \mathcal{B}(h \rightarrow \gamma\gamma) / \mathcal{B}(h \rightarrow \gamma\gamma)^{\text{SM}} = 1.02_{-0.12}^{+0.09}$ [27], that characterizes the di-photon Higgs decay modification can be written as

$$R_{\gamma\gamma} = (1 - \mathcal{B}_{BSM}) \left| 1 + \frac{v^2}{2} \frac{\sum_{j=1}^2 \frac{r_j}{m_{H_j^+}^2} A_0^{\gamma\gamma} \left(\frac{m_h^2}{4m_{H_j^+}^2} \right)}{A_1^{\gamma\gamma} \left(\frac{m_h^2}{4m_W^2} \right) + \frac{4}{3} A_{1/2}^{\gamma\gamma} \left(\frac{m_h^2}{4m_t^2} \right)} \right|^2, \quad (3.7)$$

with $r_1 = c_C^2 \omega_1 + s_C^2 \omega_2$, $r_2 = s_C^2 \omega_1 + c_C^2 \omega_2$; and \mathcal{B}_{BSM} represents any non-SM decay for the Higgs like $h \rightarrow H_i^0 H_k^0$, $A_i^0 A_k^0$. The loop functions $A_{0,1/2,1}^{\gamma\gamma}$ are given in the literature [28]. The $R_{\gamma\gamma}$ ratio estimation in (3.7) is based on the assumption of the SM production rates for the SM Higgs boson [29]. Similarly, the ratio $R_{\gamma Z} = \mathcal{B}(h \rightarrow \gamma Z) / \mathcal{B}(h \rightarrow \gamma Z)^{\text{SM}}$ can be written as

$$R_{\gamma Z} = (1 - \mathcal{B}_{BSM}) \left| 1 - \frac{v^2}{2} \frac{1 - 2s_W^2}{c_W} \frac{\sum_{j=1}^2 \frac{r_j}{m_{H_j^+}^2} A_0^{\gamma Z} \left(\frac{m_h^2}{4m_{H_j^+}^2}, \frac{m_Z^2}{4m_{H_j^+}^2} \right)}{c_W A_1^{\gamma Z} \left(\frac{m_h^2}{4m_W^2}, \frac{m_Z^2}{4m_W^2} \right) + \frac{6 - 16s_W^2}{3c_W} A_{1/2}^{\gamma Z} \left(\frac{m_h^2}{4m_t^2}, \frac{m_Z^2}{4m_t^2} \right)} \right|^2, \quad (3.8)$$

with $c_W = \cos \theta_W$, $s_W = \sin \theta_W$ and θ_W is the Weinberg mixing angle; and the loop functions $A_{0,1/2,1}^{\gamma Z}$ are given in the literature [28].

In Appendix B, we discuss the generalization of these results and constraints in the case of a n inert scalar doublets model.

4 Viable Parameter Space

In our analysis, we consider both cases where the DM candidate could be a Majorana fermion N_1 and the light inert scalar H_1^0 . By taking into account all the above mentioned theoretical and experimental constraints, we perform a full numerical scan over the model free parameters (2.8). In our scan, we consider the following ranges for the free parameters

$$|s_{H,A,C}| \leq 1, |\omega_{1,2}| < 4\pi, m_{H_1^0, A_1^0} < 3 \text{ TeV}, 78 \text{ GeV} < m_{H_1^\pm} < 3 \text{ TeV}, \quad (4.1)$$

while focusing on the parameter space regions that makes this model different than a two inert doublets model SM extension, i.e., the case with non negligible new Yukawa couplings $\min |h_{wi}| \geq 10^{-3}$.

In Fig. 2, using 4k BPs for each (scalar and Majorana) DM case, we show the mixing angles sine (left-up), the strength of the new Yukawa couplings $h_{\alpha i}$ (right-up) the masses; and the inert masses (bottom).

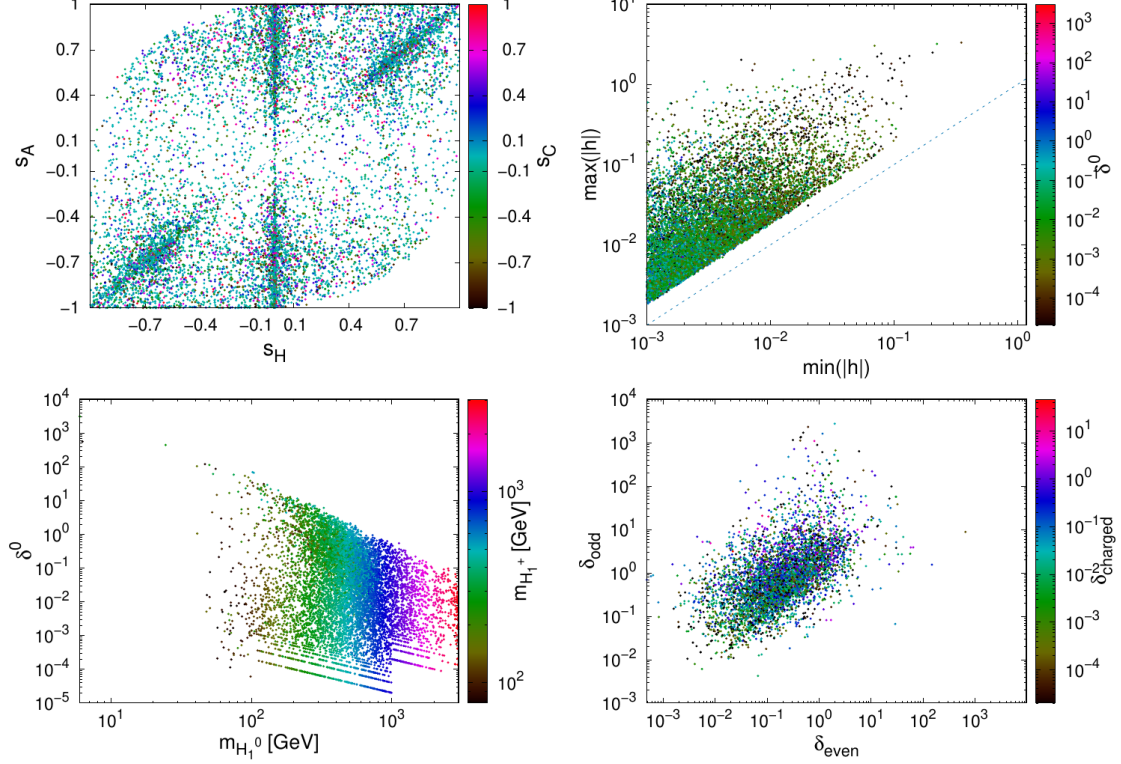


Figure 2: Left-top: the CP-even mixing angle sine vs the corresponding CP-odd one, where the palette shows the mixing of the charged scalar sector. Right-top: the strength of the new Yukawa couplings $h_{\alpha i}$ where the palette shows the ratio $\delta^0 = (m_{A_1^0}^2 - m_{H_1^0}^2)/m_{H_1^0}^2$. Left-bottom: the mass ratio $\delta^0 = (m_{A_1^0}^2 - m_{H_1^0}^2)/m_{H_1^0}^2$ versus the light CP-even scalar mass $m_{H_1^0}^2$, where the palette shows the light charged scalar mass $m_{H_1^\pm}^2$. Right-bottom: the ratios $\delta_{\text{even}} = (m_{H_2^0}^2 - m_{H_1^0}^2)/m_{H_1^0}^2$, $\delta_{\text{even}} = (m_{A_2^0}^2 - m_{A_1^0}^2)/m_{A_1^0}^2$ and $\delta_{\text{charged}} = (m_{H_2^\pm}^2 - m_{H_1^\pm}^2)/m_{H_1^\pm}^2$ that represent the mass relative difference in each sector.

Clearly from Fig. 2, the mixing angles of the CP-even, CP-odd and charged sectors can take most of the possible ranges, however, there some preferred values around $s_H = 0$ and $s_A = s_H$. All the above mentioned constraints together with the neutrino oscillation data that are taken into account via (2.17); lead to the new Yukawa couplings $h_{\alpha i}$ strength as shown in Fig. 2-top-right. It is clear that all the couplings can suppressed which makes the LFV constraints easily fulfilled and the model indistinguishable from the SM extended by two inert singlets. As mentioned previously, here we are interested in the opposite case where $|h_{\alpha i}| \geq 10^{-3}$, then, the couplings can be large as $|h_{\alpha i}| < \sqrt{4\pi}$ and a significant

hierarchy between the largest and smallest couplings strength does exist as $\max(|h_{\alpha i}|) > 1.8 \min(|h_{\alpha i}|)$. According to Fig. 2-bottom, the masses of the inert eigenstates lie within large values intervals.

In Fig. 3, we present the Higgs decay modifiers of $h \rightarrow \gamma\gamma, \gamma Z$ (left) and the oblique parameters (right).

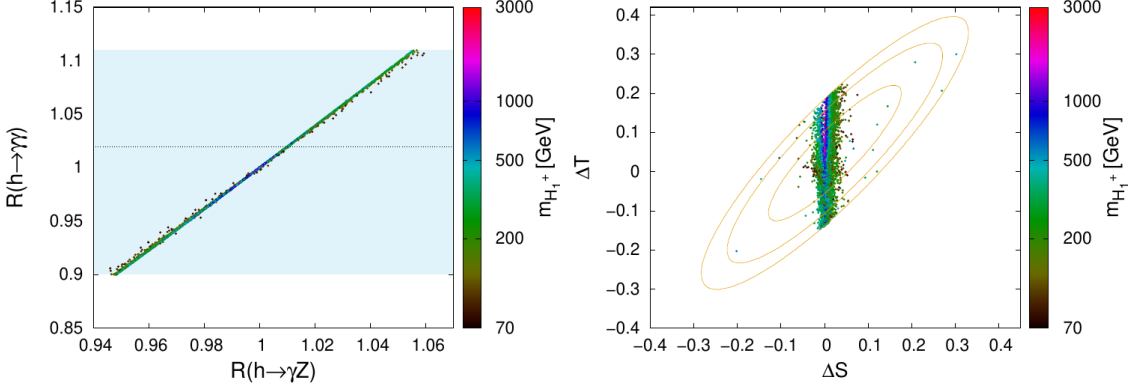


Figure 3: Left: The Higgs decay modifiers of $h \rightarrow \gamma\gamma, \gamma Z$, where the colored band represents the allowed experimental values. Right: the oblique parameters ΔT vs ΔS , where the palette shows the light charged scalar mass.

One notices that for allowed values for the Higgs branching ratio $h \rightarrow \gamma\gamma$, the branching ratio $h \rightarrow \gamma Z$ can be modified with respect to the SM within the range $[-5.2\%, 5, 1\%]$. Concerning the electroweak precision tests, as it is expected the T parameter is more sensitive to the quantum corrections due to the interactions of the gauge bosons to the two extra doublets, while the S parameter is sensitive to the corrections only in case of light charged scalars.

In Fig. 4, we show the branching ratios for the LFV processes $\ell_\alpha \rightarrow \ell_\beta + \gamma$ compared by their experimental bounds.

Like in many models, the constraint from the branching ratio $\mu \rightarrow e\gamma$ is the most severe one and the bounds from the other LFV decays ($\tau \rightarrow e\gamma$ and $\tau \rightarrow \mu\gamma$) are at least three orders of magnitude smaller.

At colliders, the model may predict many interesting signatures. For instance, it predicts all the signatures relevant to the MSctM [11]. At the LHC, charged scalars can be pair produced as $pp \rightarrow H_{1,2}^+ H_{1,2}^-$ or associated with neutral inert scalars $pp \rightarrow H_{1,2}^\pm H_{1,2}^0, H_{1,2}^\pm A_{1,2}^0$. These channels can be probed via the final states mono-lepton $\ell + \cancel{E}_T$ and di-lepton $2\ell + \cancel{E}_T$ in case if the channels $H_1^\pm \rightarrow W^\pm H_{1,2}^0, W^\pm A_{1,2}^0$ are closed. If these channels are open, then the final states $4 jets + \cancel{E}_T$ and $1\ell + 2 jets + \cancel{E}_T$ could be useful to probe this model as it is useful to probe the MSctM [11]. In order to look for beyond MSctM signatures, one has to consider the heavy inert scalar production at the LHC: $pp \rightarrow H_2^\pm H_{1,2}^\mp, H_2^\pm H_{1,2}^0, H_2^\pm A_{1,2}^0$,

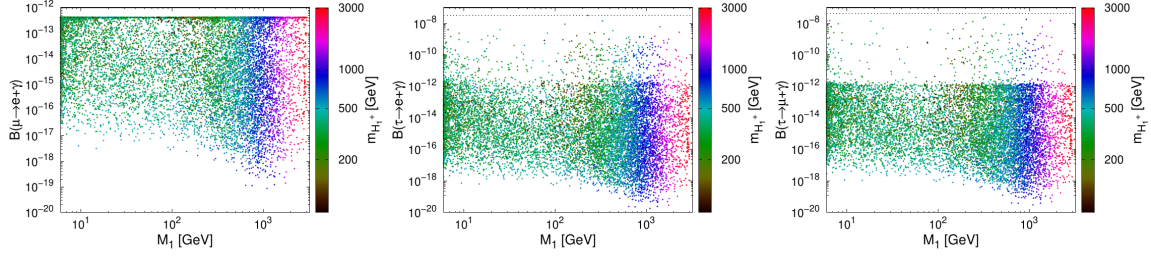


Figure 4: The branching ratio of the LFV processes $\mu \rightarrow e + \gamma$, $\tau \rightarrow e + \gamma$ and $\tau \rightarrow \mu + \gamma$ versus the light Majorana singlet fermion, where the palette shows the light charged scalar mass. The dashed horizontal line in each panel represents the branching ratio experimental bounds.

$H_2^0 H_{1,2}^\pm$, $A_2^0 H_{1,2}^\pm$, $H_2^0 H_{1,2}^0$, $A_2^0 H_{1,2}^0$, $A_2^0 A_{1,2}^0$, where the heavy scalars should decay as $H_2^+ \rightarrow W^+ H_1^0$, $W^+ A_1^0$, $h H_1^+$, $H_2^0 \rightarrow Z A_1^0$, $h H_1^0$ and $A_2^0 \rightarrow Z H_1^0$, $h A_1^0$. These novel signatures can be probed through the final states $8 \text{ jets} + \cancel{E}_T$, $1\ell + 4 \text{ jets} + \cancel{E}_T$, $1\ell + 2 \text{ jets} + \cancel{E}_T$, $4b + \cancel{E}_T$, $2 \text{ jets} + 2b + \cancel{E}_T$, $2b + \cancel{E}_T$, that may not be seen in the MSctM or in other neutrino mass and DM motivated SM extensions. The investigation of these novel signatures requires a full and precise numerical scan to define the relevant regions of the parameter space, that should be confronted with the existing analyses.

5 Dark Matter: Majorana or Scalar?

In this model, DM candidate could be either the light Majorana fermion (N_1), the light CP -even (CP -odd) scalar H_1^0 (A_1^0), or a mixture of all these components if they are degenerate in mass. In the case of scalar DM, the possible annihilation channels are $W^\pm W^\mp$, ZZ , $q_i \bar{q}_i$, hh , $\bar{\ell}_\alpha \ell_\beta$ and $\bar{\nu}_\alpha \nu_\beta$. In this case, very small couplings $h_{\alpha i}$ could be favored by the LFV constraints, and therefore the contributions of the channels $\nu_\alpha \bar{\nu}_\beta$, $\ell_\alpha \ell_\beta$ to the annihilation cross section would be negligible. Then, this case is almost identical to the SM extended by two inert doublets with scalar DM. The co-annihilation effect along the channels $H_1^0 A_1^0 (A_1^0 A_1^0) \rightarrow X_{SM} X'_{SM}$ could be important if the mass difference $(m_{A_1^0}^2 - m_{H_1^0}^2) / (m_{A_1^0}^2 + m_{H_1^0}^2)$ is small enough. This makes the couplings $h_{\alpha i}$ non-suppressed and therefore the annihilation into $\nu_\alpha \bar{\nu}_\beta$, $\ell_\alpha \ell_\beta$ is more important. Such effect could make this setup (spin-0 DM) better than the minimal IDM. In case of Majorana DM scenario, the DM (co-)annihilation could occur into charged leptons $\ell_\alpha^- \ell_\beta^+$ and light neutrinos $\nu_\alpha \bar{\nu}_\beta$; via t -channel diagrams mediated by the charged scalar $H_{1,2}^\pm$; and the neutral scalars $H_{1,2}^0$, $A_{1,2}^0$, respectively. Here, the annihilation cross section is fully triggered by the non-suppressed values of the couplings $h_{\alpha i}$.

In case of scalar DM, negative searches from DM direct detection (DD) at underground detectors impose more constraints on the parameters space. This is translated into upper bounds on the DM-nucleon cross section. In our model, the DM interaction with nucleons occurs via a single t-channel diagram mediated by the Higgs, and the scattering cross-section is given by³

$$\sigma_{det} = \frac{(\lambda_{hH_1^0 H_1^0})^2}{4\pi v^2 m_h^4} \frac{m_{\mathcal{N}}^2 (m_{\mathcal{N}} - \frac{7}{9} m_B)^2}{(m_{\mathcal{N}} + m_{H_1^0})^2}, \quad (5.1)$$

where $m_{\mathcal{N}}$ and m_B are, respectively, the nucleon and baryon masses in the chiral limit [30]; and $\lambda_{hH_1^0 H_1^0} = \frac{v}{2} [c_H^2 (\kappa_1 + \omega_1 + \zeta_1) + s_H^2 (\kappa_2 + \omega_2 + \zeta_2) + 2s_H c_H (\zeta_3 + \zeta_4)]$ is the DM Higgs triple coupling. In Fig. 5, we show the DD cross section (5.1) versus the DM mass for the BPs used in Fig. 2 that correspond to scalar DM cases, compared with recent experimental bounds from the PandaX-4T experiment [31] and LUX-ZEPLIN [16].

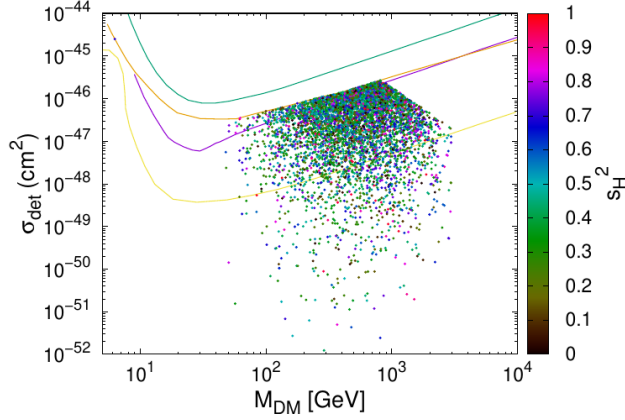


Figure 5: The DD cross section vs the DM mass for the scalar DM BPs used in Fig. 2. The violet, blue and orange lines correspond to the bounds from LUX-ZEPLIN [16], Xenon-1T bound [32] and PandaX-4T [31], respectively, while the yellow one represents the neutrino floor [33].

In order to show that both scalar and Majorana DM scenarios are viable in this model, we consider the two BPs among the BPs used in Fig. 2, where their free parameters values are given Table 1, where BP1 and BP2 correspond to Majorana and scalar DM cases, respectively.

³In the scalar DM scenario, the vertex $ZH_1^0 H_1^0$ is vanishing since violates CP symmetry. However, the vertex $ZH_1^0 A_1^0$ does not vanish, but the process $H_1^0 \mathcal{N} \rightarrow A_1^0 \mathcal{N}$ is kinematically forbidden. In case of Majorana DM, the vertex $hN_1 N_1$ ($ZN_1 N_1$) is vanishing at tree-level due to the fact that the fermion N_1 is a singlet (a Majorana one). At loop level, it has been shown that DD cross section is few orders of magnitude suppressed [11, 37].

BP1	$s_{H,A,C} = \{-0.053734, 0.72187, 0.82912\}$, $\omega_{1,2} = \{-0.15715, -0.92515\}$, $m_{H_1^0} = \{2755.6, 2820.6\}$, $m_{A_1^0} = \{2766.7, 2823\}$, $m_{H_{1,2}^\pm} = \{2318.7, 2327.8\}$, $M_i = \{2317.1, 2318.7, 2327.8\}$, $h_{\alpha i} = \begin{pmatrix} -1.3664 - i0.066927, & -0.0063156 - i1.1746, & -0.020184 + i0.28501, & -0.0063503 - i1.1811, & -1.3739 - i0.067294, & -0.020295 + i0.28657 \\ 1.8625 + i0.046833, & -0.09083 - i2.2339, & -0.0063982 - i0.33045, & -0.091329 - i2.2461, & 1.8727 + i0.04709, & -0.0064333 - i0.33226 \\ -2.4404 - i0.065694, & -0.667 - i1.8413, & 0.037294 - i0.36281, & -0.67066 - i1.8514, & -2.4538 - i0.066055, & 0.037499 - i0.36481 \end{pmatrix}$
BP2	$s_{H,A,C} = \{-0.38546, -0.27092, -0.019603\}$, $\omega_{1,2} = \{-1.0362, 5.1668\}$, $m_{H_1^0} = \{1228.9, 1246\}$, $m_{A_1^0} = \{1229.3, 1266\}$, $m_{H_{1,2}^\pm} = \{1230.4, 1270.1\}$, $M_i = \{1633.4, 1850.7, 1853.5\}$, $h_{\alpha i} = 10^{-3} \times \begin{pmatrix} 2.5475 - i51.865, & 15.027 + i1.4322, & 19.457 + i0.69002, & 0.44292 - i9.0175, & 2.6139 + i0.24914, & 3.3845 + i0.12003 \\ -1.7657 + i70.885, & -31.844 + i0.82879, & 4.9703 - i0.46673, & -0.307 + i12.325, & -5.5394 + i0.14417, & 0.86461 - i0.08119 \\ 2.5076 - i92.163, & -33.608 + i0.041734, & 1.0967 - i6.4609, & 0.43599 - i16.024, & -5.8463 + i0.0072598, & 0.19077 - i1.1239 \end{pmatrix}$

Table 1: The values of the free parameters for BP1 and BP2. Here, all the masses are given in GeV.

Then, we use the package MadDM [34] to estimate the relic density and the direct detection cross section for the scalar DM case by varying both the DM mass and the Yukawa couplings $h_{\alpha i}$ strength as shown in Fig. 6. In order to do so, we used the package FeynRules [35] to implement the model and produce the UFO files [36].

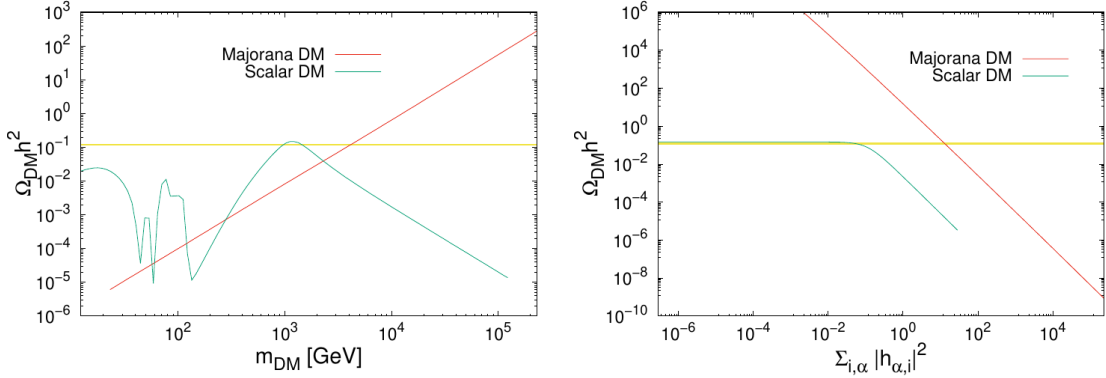


Figure 6: The DM relic density versus the DM mass (left) and versus the couplings combination $\sum_{i,\alpha} |h_{\alpha,i}|^2$ (right). The yellow band represents the observed the DM relic density value. One has to mention that in the left panel, we make all masses changing simultaneously, i.e., all the mass fulfill the condition $m_i/m_{DM} = \text{constant}$ with all the DM mass interval.

According to Fig. 6, it is clear that the right amount of the DM relic density can be achieved in this model whether the DM is a Majorana or a scalar particle. From Fig. 6-left, the dependence of the relic density on the DM mass in case of Majorana DM seems to be quadratic $\Omega_{DM} h^2 \sim m_{DM}^2$ (or $\sigma_{DM} \sim 1/m_{DM}^2$). This can be understood due to the fact that the Majorana DM (co-)annihilation occurs via simple channels, i.e., $N_1 N_1 (N_{2,3}) \rightarrow \nu_\alpha \bar{\nu}_\beta, \ell_\alpha \bar{\ell}_\beta$. However, in the scalar DM case, its dependence on the DM mass is not trivial due to the existence of many annihilation channels ($N_1 N_1 (N_{2,3}) \rightarrow W^\pm W^\mp, ZZ, q_i \bar{q}_i, hh$,

$\bar{\ell}_\alpha \ell_\beta$ and $\bar{\nu}_\alpha \nu_\beta$), where each channel could be dominant within a specific DM mass range. From Fig. 6-right, one learns that in the scalar DM case the DM annihilation into $\nu_\alpha \bar{\nu}_\beta, \ell_\alpha \ell_\beta$ could be efficient only if $\sum_{i,\alpha} |h_{\alpha,i}|^2 \sim 0.1$. However, since the DM is annihilated only via the channels $\nu_\alpha \bar{\nu}_\beta, \ell_\alpha \ell_\beta$ for the Majorana DM case, the Yukawa coupling magnitude is very important, and it is solely dictated by the relic density right amount. Therefore, Yukawa couplings of order $\mathcal{O}(0.1 \sim 1)$ could be problematic for the LFV constraints. In order to fulfill the requirements of DM relic density, the LFV constraints and the neutrino oscillation data together, one has to impose that the six terms in the summation in (3.5) should cancel together. Although, this is not surprising since it has been shown in the MSctM with Majorana DM [11] that these requirements are fulfilled by the imposing the cancellation of three terms in a formula similar to (3.5); for a large DM mass range. Indeed, in our model, the Feynman diagrams relevant to the neutrino mass, LFV and DM annihilation are more numerous; and involve more free parameters with respect the MSctM, and hence make the DM relic density, the LFV constraints and the neutrino oscillation data easily relaxed with respect to the case in [11].

6 Conclusion

In this paper, we proposed a SM extension by three singlet Majorana fermions and two scalar inert doublets. After diagonalizing the scalar squared mass sub-matrices, we found that the model includes two CP-even ($H_{1,2}^0$), two CP-odd ($A_{1,2}^0$) and two charged scalar ($H_{1,2}^\pm$) eigenstates, with different mixing angles. Then, the values of many physical observables got modified with respect to the MSctM. For instance, the neutrino mass is generated at one-loop level via 12 diagrams instead of 6 in the MSctM. Similar remarks hold for the observables relevant to the electroweak precision tests, LFV and the di-photon Higgs decay, where many masses and mixing angles are included. This made the neutrino oscillation data easily explained without being in conflict with the different theoretical and experimental constraints for large parameter space regions.

The dark matter (DM) in this model could be either fermionic (N_1) or scalar (the lightest among H_1^0 and A_1^0). We have shown that the right amount of the relic density can be easily achieved in both scenarios for different DM mass ranges. In addition, for the scalar DM scenario the model can accommodate the constraints for the direct detection cross section of the DM-nucleon scattering.

The model predicts all the signatures predicted by the MSctM, however, novel signature relevant to the production and decay of the heavy scalars (H_2^\pm, H_2^0, A_2^0) can be probed through some final states like: $8 \text{ jets} + \cancel{E}_T$, $1\ell + 4 \text{ jets} + \cancel{E}_T$, $1\ell + 2 \text{ jets} + \cancel{E}_T$, $4b + \cancel{E}_T$, $2 \text{ jets} + 2b + \cancel{E}_T$ and $2b + \cancel{E}_T$. This point requires an independent investigation.

Acknowledgments

This work is funded by the University of Sharjah under the research projects No 21021430100 “Extended Higgs Sectors at Colliders: Constraints & Predictions” and No 21021430107 “Hunting for New Physics at Colliders”.

A Generalized Casas-Ibarra parameterization

It is well known that a (complex) 3×3 fermionic mass matrices can be diagonalized via two unitary matrices U and V à la singular decomposition value problem [38], as

$$m^{(v)} = U \cdot D_m \cdot V^\dagger, \quad (\text{A.1})$$

with $D_m = \text{diag}\{m_1, m_2, m_3\}$. Here, $U_{3 \times 3}$ and $V_{3 \times 3}$ can be defined as the unitary matrices that diagonalize the matrices products $m^{(v)} \cdot (m^{(v)})^\dagger$ and $(m^{(v)})^\dagger \cdot m^{(v)}$, respectively. In other words $U^\dagger \cdot [m^{(v)} \cdot (m^{(v)})^\dagger] \cdot U = D_m^\dagger \cdot D_m = D_{m^2} = D_m \cdot D_m^\dagger = V^\dagger \cdot [(m^{(v)})^\dagger \cdot m^{(v)}] \cdot V$. In the case of neutrino Majorana mass, the matrix (A.1) is complex symmetric, which implies $U = V^*$ and therefore

$$m^{(v)} = U \cdot D_m \cdot U^T. \quad (\text{A.2})$$

This allows to write a general form for the diagonal matrix D_m as

$$D_m = \mathcal{P}_1 \cdot U^T \cdot m^{(v)} \cdot U \cdot \mathcal{P}_2, \quad (\text{A.3})$$

where the matrices $\mathcal{P}_{1,2} = \text{diag}\{1, e^{i\zeta_{1,2}}, e^{i\vartheta_{1,2}}\}$ can be absorbed in a redefinition of the Majorana phase matrix in the PNMS mixing matrix; and similarly, D_m in (A.3) can be converted to a diagonal matrix with real positive elements. This parameterization (A.3) is in agreement with the so-called Takagi diagonalization [39].

In what follows, we consider the new Yukawa couplings are given by the matrix $h_{3,M}$, with $M = 3n$ and is the inert doublets number that are considered in the scotogenic model generalization. In this case, the matrix Λ in (2.14) should be a $M \times M$ matrix rather than 6×6 one. In our case, we have $n = 2$ and then the Yukawa couplings are presented by 3×6 complex matrix. Following the Casas-Ibarra approach [19], the Yukawa couplings are assumed to have the form of a product of many matrices as

$$h = S_1 \cdot S_2 \cdot S_3 \cdot S_4 \cdot S_5. \quad (\text{A.4})$$

Then by replacing (A.4) in (2.14); and match it with (A.2), one immediately finds that $S_1 = U_{3 \times 3}$ is the 3×3 PNMS mixing matrix. In order to identify the remaining matrices, we simplify the product $U^\dagger \cdot m^{(v)} \cdot (m^{(v)})^\dagger \cdot U$ and match it with D_{m^2} . Then, in case where the matrix $S_5 = Q$ is chosen to be the orthogonal $M \times M$ matrix that diagonalizes the symmetric real matrix Λ as $Q_{M \times M} \cdot (\Lambda)_{M \times M} \cdot Q_{M \times M}^T = D_{\Lambda'} = \text{diag}\{\Lambda'_1, \Lambda'_2, \dots, \Lambda'_M\}$; and the matrix

S_4 to be the diagonal $M \times M$ matrix $S_4 = D_{(\Lambda')^{-1/2}} = \text{diag}\{(\Lambda'_1)^{-1/2}, (\Lambda'_2)^{-1/2}, \dots, (\Lambda'_M)^{-1/2}\}$, then the product $U^\dagger \cdot m^{(v)} \cdot (m^{(v)})^\dagger \cdot U$ can be written as

$$U^\dagger \cdot m^{(v)} \cdot (m^{(v)})^\dagger \cdot U = (S_2 \cdot S_3)_{3 \times M} \cdot (S_3^T \cdot S_2^T)_{M \times 3} \cdot (S_2^* \cdot S_3^*)_{3 \times M} \cdot (S_3^\dagger \cdot S_2^\dagger)_{M \times 3}. \quad (\text{A.5})$$

Here, Λ'_i are the eigenvalues of the matrix Λ . In order to match (A.5) with D_{m^2} , it is enough to have $S_2 = D_{m^{1/2}} = \text{diag}\{m_1^{1/2}, m_2^{1/2}, m_3^{1/2}\}$ and $S_3 = T$ with $(T)_{3 \times M} \cdot (T^T)_{M \times 3} = \mathbf{1}_{3 \times 3}$. Obviously, for $M = 3$ the matrix T is just a 3×3 orthogonal matrices $T \cdot T^T = T^T \cdot T = \mathbf{1}_{3 \times 3}$. However, for $M = 3 \times k$, we claim that the matrix T has the most general form

$$T_{3 \times (3k)} = (\alpha^{(1)} R_{3 \times 3}^{(1)}, \alpha^{(2)} R_{3 \times 3}^{(2)}, \dots, \alpha^{(k)} R_{3 \times 3}^{(k)}), \quad (\text{A.6})$$

with $R^{(i)}$ are 3×3 orthogonal matrices $R^{(i)} \cdot (R^{(i)})^T = (R^{(i)})^T \cdot R^{(i)} = \mathbf{1}_{3 \times 3}$, and $\alpha^{(i)}$ are real numbers that fulfill the identity $\sum_i (\alpha^{(i)})^2 = 1$.

In order to get large Yukawa couplings as favored by collider searches or required by Majorana DM relic density, it is enough to choose a diagonalization matrix $(Q)_{M \times M}$ that leads to the order $|\Lambda'_1| < |\Lambda'_2| < \dots < |\Lambda'_M|$; and $\alpha^{(1)} = 1, \alpha^{(i>1)} = 0$.

B Scotogenic Model with n inert Doublets

In case of a scotogenic model with N inert doublets $(\Phi_{i=1,n})$ with the global Z_2 symmetry $N_i \rightarrow -N_i, \Phi_i \rightarrow -\Phi_i$, the Lagrangian (2.1) can be generalized as

$$\mathcal{L} \supset \sum_{i=1}^n \sum_{k=1}^3 \bar{L}_\alpha ((h_{\alpha,k+3(i-1)}) \epsilon \Phi_i) N_k + \frac{1}{2} \bar{N}_k^C M_k N_k + h.c., \quad (\text{B.1})$$

where the new Yukawa couplings $h_{\alpha,i}$ here are a $3 \times (3n)$ matrix. The scalar potential (2.2) can be generalized as

$$\begin{aligned} V(\mathcal{H}, \Phi_i, S, \chi) = & -\mu_H^2 |\mathcal{H}|^2 + \mu_i^2 |\Phi_i|^2 + \frac{\lambda_H}{6} |\mathcal{H}|^4 + \frac{\lambda_i}{6} |\Phi_i|^4 + \omega_i |\mathcal{H}|^2 |\Phi_i|^2 + \kappa_i |\mathcal{H}^\dagger \Phi_i|^2 \\ & + \varrho_{i,j}^{(1)} |\Phi_i|^2 |\Phi_j|^2 + \varrho_{i,j}^{(2)} |\Phi_i^\dagger \Phi_j|^2 + \left\{ \mu_{3,ij}^2 \Phi_i^\dagger \Phi_j + \frac{1}{2} \zeta_i^{(1)} (\mathcal{H}^\dagger \Phi_i)^2 \right. \\ & \left. + \zeta_{i,j}^{(2)} (\mathcal{H}^\dagger \Phi_i) (\mathcal{H}^\dagger \Phi_j) + \zeta_{i,j}^{(3)} (\Phi_i^\dagger \mathcal{H}) (\mathcal{H}^\dagger \Phi_j) + h.c. \right\}. \quad (\text{B.2}) \end{aligned}$$

In case of CP-conservation (real values of all potential parameters), there are n charged eigenstates $(H_{j=1,n}^\pm)$, n neutral CP-even eigenstates $(H_{j=1,n}^0)$ and n neutral CP-odd eigenstates $(A_{j=1,n}^0)$ with similar couplings to (2.11). In (2.11), the mixing $(c_{H,A,C}$ and $s_{H,A,C}$ should be replaced by the elements of the mixing matrices $\mathcal{U}^{(H,A,C)}$ that diagonalize the CP-even, CP-odd and charged scalars squared $n \times n$ mass matrices, respectively, where the summation should be performed over $j = 1, n$. Consequently, the neutrino mass is generated via $4 \times n$ diagrams mediated by $N_{1,2,3}$ and $H_{j=1,n}^0 / A_{j=1,n}^0$. Therefore, the formulas of the mass matrix elements (2.12) and the values of the new Yukawa couplings

in (2.17) hold for $j = 1, n$ and $M = 3 \times n$. Similar conclusions can be achieved for the LFV branching ratios (3.5) and the di-photon Higgs decay ratio (3.7). For the oblique parameters (3.6), the summation should be performed over $j = 1, n$; and the mixing ($c_{H,A,C}$ and $s_{H,A,C}$) should be replaced by the elements of the mixing matrix $\mathcal{U}^{(H,A,C)}$. By considering n_N Majorana singlet fermions instead of three, the description of this generalization corresponds what called the *general scotogenic model* [14].

C The Unitarity Amplitude Matrices

Here, we give the relevant amplitude matrices for the unitarity. We have the following basis that characterize the initial/final states:

CP-even, Z_2 even, & $Q_{em} = 0$: the basis is $\{hh, \chi^0\chi^0, S_1^0S_1^0, S_2^0S_2^0, Q_1^0Q_1^0, Q_2^0Q_2^0, \chi^+\chi^-, S_1^+S_1^-, S_2^+S_2^-, S_1^+S_2^-\}$; and the matrix is

$$\begin{bmatrix} \lambda_H, & \frac{1}{3}\lambda_H, & \omega_1 + \kappa_1 + \tilde{\zeta}_1, \omega_2 + \kappa_2 + \tilde{\zeta}_2, \omega_1 + \kappa_1 - \tilde{\zeta}_1, \omega_2 + \kappa_2 - \tilde{\zeta}_2, & \frac{1}{3}\lambda_H, & \omega_1, & \omega_2, & 0 \\ \frac{1}{3}\lambda_H, & \lambda_H, & \omega_1 + \kappa_1 - \tilde{\zeta}_1, \omega_2 + \kappa_2 - \tilde{\zeta}_2, \omega_1 + \kappa_1 + \tilde{\zeta}_1, \omega_2 + \kappa_2 + \tilde{\zeta}_2, & \frac{1}{3}\lambda_H, & \omega_1, & \omega_2, & 0 \\ \omega_1 + \kappa_1 + \tilde{\zeta}_1, \omega_1 + \kappa_1 - \tilde{\zeta}_1, & \lambda_1, & \varrho_1 + \varrho_2, & \frac{1}{3}\lambda_1, & \varrho_1 + \varrho_2, & \omega_1, & \frac{1}{3}\lambda_1, & \varrho_1, & 0 \\ \omega_2 + \kappa_2 + \tilde{\zeta}_2, \omega_2 + \kappa_2 - \tilde{\zeta}_2, & \varrho_1 + \varrho_2, & \lambda_2, & \varrho_1 + \varrho_2, & \frac{1}{3}\lambda_2, & \omega_2, & \varrho_1, & \frac{1}{3}\lambda_2, & 0 \\ \omega_1 + \kappa_1 - \tilde{\zeta}_1, \omega_1 + \kappa_1 + \tilde{\zeta}_1, & \frac{1}{3}\lambda_1, & \varrho_1 + \varrho_2, & \lambda_1, & \varrho_1 + \varrho_2, & \omega_1, & \frac{1}{3}\lambda_1, & \varrho_1, & 0 \\ \omega_2 + \kappa_2 - \tilde{\zeta}_2, \omega_2 + \kappa_2 + \tilde{\zeta}_2, & \varrho_1 + \varrho_2, & \frac{1}{3}\lambda_2, & \varrho_1 + \varrho_2, & \lambda_2, & \omega_2, & \varrho_1, & \frac{1}{3}\lambda_2, & 0 \\ \frac{1}{3}\lambda_H, & \frac{1}{3}\lambda_H, & \omega_1, & \omega_2, & \omega_1, & \omega_2, & \frac{2}{3}\lambda_H, & \kappa_1 + \omega_1, \kappa_2 + \omega_2, & \tilde{\zeta}_4 \\ \omega_1, & \omega_1, & \frac{1}{3}\lambda_1, & \varrho_1, & \frac{1}{3}\lambda_1, & \varrho_1, & \kappa_1 + \omega_1, & \frac{2}{3}\lambda_1, & \varrho_1 + \varrho_2, & 0 \\ \omega_2, & \omega_2, & \varrho_1, & \frac{1}{3}\lambda_2, & \varrho_1, & \frac{1}{3}\lambda_2, & \kappa_2 + \omega_2, & \varrho_1 + \varrho_2, & \frac{2}{3}\lambda_2, & 0 \\ 0, & 0, & 0, & 0, & 0, & 0, & \tilde{\zeta}_4, & 0, & 0, & \varrho_1 + \varrho_2 \end{bmatrix} \quad (\text{C.1})$$

CP-even, Z_2 even, & $Q_{em} = 0$: the basis is $\{hS_1^0, hS_2^0, \chi^0Q_1^0, \chi^0Q_2^0, \chi^+S_1^-, \chi^+S_2^-\}$; and the matrix is

$$\begin{bmatrix} \omega_1 + \kappa_1 + \tilde{\zeta}_1, & \tilde{\zeta}_3 + \tilde{\zeta}_4, & \tilde{\zeta}_1, & \tilde{\zeta}_3, & \frac{1}{2}(\kappa_1 + \tilde{\zeta}_1), & \frac{1}{2}(\tilde{\zeta}_3 + \tilde{\zeta}_4) \\ \tilde{\zeta}_3 + \tilde{\zeta}_4, & \omega_2 + \kappa_2 + \tilde{\zeta}_2, & \tilde{\zeta}_3, & \tilde{\zeta}_2, & \frac{1}{2}(\tilde{\zeta}_3 + \tilde{\zeta}_4), & \frac{1}{2}(\kappa_2 + \tilde{\zeta}_2) \\ \tilde{\zeta}_1, & \tilde{\zeta}_3, & \omega_1 + \kappa_1 + \tilde{\zeta}_1, & \tilde{\zeta}_3 + \tilde{\zeta}_4, & \frac{1}{2}(\kappa_1 + \tilde{\zeta}_1), & \frac{1}{2}(\tilde{\zeta}_3 + \tilde{\zeta}_4) \\ \tilde{\zeta}_3, & \tilde{\zeta}_2, & \tilde{\zeta}_3 + \tilde{\zeta}_4, & \omega_2 + \kappa_2 + \tilde{\zeta}_2, & \frac{1}{2}(\tilde{\zeta}_3 + \tilde{\zeta}_4), & \frac{1}{2}(\kappa_2 + \tilde{\zeta}_2) \\ \frac{1}{2}(\kappa_1 + \tilde{\zeta}_1), & \frac{1}{2}(\tilde{\zeta}_3 + \tilde{\zeta}_4), & \frac{1}{2}(\kappa_1 + \tilde{\zeta}_1), & \frac{1}{2}(\tilde{\zeta}_3 + \tilde{\zeta}_4), & \kappa_1 + \omega_1, & \tilde{\zeta}_4 \\ \frac{1}{2}(\tilde{\zeta}_3 + \tilde{\zeta}_4), & \frac{1}{2}(\kappa_2 + \tilde{\zeta}_2), & \frac{1}{2}(\tilde{\zeta}_3 + \tilde{\zeta}_4), & \frac{1}{2}(\kappa_2 + \tilde{\zeta}_2), & \tilde{\zeta}_4, & \kappa_2 + \omega_2 \end{bmatrix} \quad (\text{C.2})$$

CP-even, Z_2 even, & $Q_{em} = 0$: the basis is $\{h\chi^0, S_1^0Q_1^0, S_1^0Q_2^0, S_2^0Q_1^0, S_2^0Q_2^0, \chi^+\chi^-, S_1^+S_1^-,$

$S_2^+ S_2^-, S_1^+ S_2^-$ }; and the matrix is

$$\begin{bmatrix} \frac{1}{3}\lambda_H, & \zeta_1, & \zeta_3, & \zeta_3, & \zeta_2, & 0, & 0, & 0, & 0 \\ \zeta_1, & \frac{1}{3}\lambda_1, & 0, & 0, & 0, & 0, & 0, & 0, & 0 \\ \zeta_3, & 0, & \varrho_1 + \varrho_2, & 0, & 0, & 0, & 0, & 0, & -\frac{i}{2}\varrho_2 \\ \zeta_3, & 0, & 0, & \varrho_1 + \varrho_2, & 0, & 0, & 0, & 0, & \frac{i}{2}\varrho_2 \\ \zeta_2, & 0, & 0, & 0, & \frac{1}{3}\lambda_2, & 0, & 0, & 0, & 0 \\ 0, & 0, & 0, & 0, & 0, & \frac{2}{3}\lambda_H, & \kappa_1 + \omega_1, & \kappa_2 + \omega_2, & \zeta_4 \\ 0, & 0, & 0, & 0, & 0, & \kappa_1 + \omega_1, & \frac{2}{3}\lambda_1, & \varrho_1 + \varrho_2, & 0 \\ 0, & 0, & 0, & 0, & 0, & \kappa_2 + \omega_2, & \varrho_1 + \varrho_2, & \frac{2}{3}\lambda_2, & 0 \\ 0, & 0, & \frac{i}{2}\varrho_2, & -\frac{i}{2}\varrho_2, & 0, & \zeta_4, & 0, & 0, & \varrho_1 + \varrho_2 \end{bmatrix} \quad (\text{C.3})$$

CP-even, Z_2 even, & $Q_{em} = 0$: the basis is $\{hQ_1^0, hQ_2^0, S_1^0\chi^0, S_2^0\chi^0, \chi^+ S_1^-, \chi^+ S_2^-\}$; and the matrix is

$$\begin{bmatrix} \omega_1 + \kappa_1 - \zeta_1, & -\zeta_3 + \zeta_4, & \zeta_1, & \zeta_3, & -\frac{i}{2}(\kappa_1 - \zeta_1), & \frac{i}{2}(\zeta_3 - \zeta_4) \\ -\zeta_3 + \zeta_4, & \omega_2 + \kappa_2 - \zeta_2, & \zeta_3, & \zeta_2, & \frac{i}{2}(\zeta_3 - \zeta_4), & -\frac{i}{2}(\kappa_2 - \zeta_2) \\ \zeta_1, & \zeta_3, & \omega_1 + \kappa_1 - \zeta_1, & -\zeta_3 + \zeta_4, & \frac{i}{2}(\kappa_1 - \zeta_1), & -\frac{i}{2}(\zeta_3 - \zeta_4) \\ \zeta_3, & \zeta_2, & -\zeta_3 + \zeta_4, & \omega_2 + \kappa_2 - \zeta_2, & -\frac{i}{2}(\zeta_3 - \zeta_4), & \frac{i}{2}(\kappa_2 - \zeta_2) \\ \frac{i}{2}(\kappa_1 - \zeta_1), & -\frac{i}{2}(\zeta_3 - \zeta_4), & -\frac{i}{2}(\kappa_1 - \zeta_1), & \frac{i}{2}(\zeta_3 - \zeta_4), & \kappa_1 + \omega_1, & \zeta_4 \\ -\frac{i}{2}(\zeta_3 - \zeta_4), & \frac{i}{2}(\kappa_2 - \zeta_2), & \frac{i}{2}(\zeta_3 - \zeta_4), & -\frac{i}{2}(\kappa_2 - \zeta_2), & \zeta_4, & \kappa_2 + \omega_2 \end{bmatrix} \quad (\text{C.4})$$

CP-even, Z_2 even, & $Q_{em} = 0$: the basis is $\{h\chi^+, \chi^0\chi^+, S_1^0 S_1^+, S_1^0 S_2^+, S_2^0 S_1^+, S_2^0 S_2^+, Q_1^0 S_1^+, Q_1^0 S_2^+, Q_2^0 S_1^+, Q_2^0 S_2^+\}$; and the matrix is

$$\begin{bmatrix} \frac{1}{3}\lambda_H, & 0, & \frac{1}{2}(\kappa_1 + \zeta_1), & \frac{1}{2}(\zeta_3 + \zeta_4), & \frac{1}{2}(\zeta_3 + \zeta_4), & \frac{1}{2}(\kappa_2 + \zeta_2), & \frac{i}{2}(\kappa_1 - \zeta_1), & -\frac{i}{2}(\zeta_3 - \zeta_4), & -\frac{i}{2}(\zeta_3 - \zeta_4), & \frac{i}{2}(\kappa_2 - \zeta_2) \\ 0, & \frac{1}{3}\lambda_H, & -\frac{i}{2}(\kappa_1 - \zeta_1), & \frac{i}{2}(\zeta_3 - \zeta_4), & \frac{i}{2}(\zeta_3 - \zeta_4), & -\frac{i}{2}(\kappa_2 - \zeta_2), & \frac{1}{2}(\kappa_1 + \zeta_1), & \frac{1}{2}(\zeta_3 + \zeta_4), & \frac{1}{2}(\zeta_3 + \zeta_4), & \frac{1}{2}(\kappa_2 + \zeta_2) \\ \frac{1}{2}(\kappa_1 + \zeta_1), & \frac{i}{2}(\kappa_1 - \zeta_1), & \frac{1}{3}\lambda_1, & 0, & 0, & \frac{1}{2}\varrho_2, & 0, & 0, & 0, & \frac{i}{2}\varrho_2 \\ \frac{1}{2}(\zeta_3 + \zeta_4), & -\frac{i}{2}(\zeta_3 - \zeta_4), & 0, & \varrho_1, & \frac{1}{2}\varrho_2, & 0, & 0, & 0, & -\frac{i}{2}\varrho_2, & 0 \\ \frac{1}{2}(\zeta_3 + \zeta_4), & -\frac{i}{2}(\zeta_3 - \zeta_4), & 0, & \frac{1}{2}\varrho_2, & \varrho_1, & 0, & 0, & -\frac{i}{2}\varrho_2, & 0, & 0 \\ \frac{1}{2}(\kappa_2 + \zeta_2), & \frac{i}{2}(\kappa_2 - \zeta_2), & \frac{1}{2}\varrho_2, & 0, & 0, & \frac{1}{3}\lambda_2, & \frac{i}{2}\varrho_2, & 0, & 0, & 0 \\ -\frac{i}{2}(\kappa_1 - \zeta_1), & \frac{1}{2}(\kappa_1 + \zeta_1), & 0, & 0, & 0, & -\frac{i}{2}\varrho_2, & \frac{1}{3}\lambda_1, & 0, & 0, & \frac{1}{2}\varrho_2 \\ \frac{i}{2}(\zeta_3 - \zeta_4), & \frac{1}{2}(\zeta_3 + \zeta_4), & 0, & 0, & \frac{i}{2}\varrho_2, & 0, & 0, & \varrho_1, & \frac{1}{2}\varrho_2, & 0 \\ \frac{i}{2}(\zeta_3 - \zeta_4), & \frac{1}{2}(\zeta_3 + \zeta_4), & 0, & 0, & \frac{i}{2}\varrho_2, & 0, & 0, & 0, & \frac{1}{2}\varrho_2, & \varrho_1 \\ -\frac{i}{2}(\kappa_2 - \zeta_2), & \frac{1}{2}(\kappa_2 + \zeta_2), & -\frac{i}{2}\varrho_2, & 0, & 0, & 0, & \frac{1}{2}\varrho_2, & 0, & 0, & \frac{1}{3}\lambda_2 \end{bmatrix} \quad (\text{C.5})$$

CP-even, Z_2 even, & $Q_{em} = 0$: the basis is $\{hS_1^+, hS_2^+, \chi^0 S_1^+, \chi^0 S_2^+, S_1^0 \chi^+, S_2^0 \chi^+, Q_1^0 \chi^+, Q_2^0 \chi^+\}$; and the matrix is

$$\begin{bmatrix} \omega_1, & 0, & 0, & 0, & \frac{1}{2}(\kappa_1 + \zeta_1), & \frac{1}{2}(\zeta_3 + \zeta_4), & -\frac{i}{2}(\kappa_1 - \zeta_1), & \frac{i}{2}(\zeta_3 - \zeta_4) \\ 0, & \omega_2, & 0, & 0, & \frac{1}{2}(\zeta_3 + \zeta_4), & \frac{1}{2}(\kappa_2 + \zeta_2), & \frac{i}{2}(\zeta_3 - \zeta_4), & -\frac{i}{2}(\kappa_2 - \zeta_2) \\ 0, & 0, & \omega_1, & 0, & \frac{i}{2}(\kappa_1 - \zeta_1), & -\frac{i}{2}(\zeta_3 - \zeta_4), & \frac{1}{2}(\kappa_1 + \zeta_1), & \frac{1}{2}(\zeta_3 + \zeta_4) \\ 0, & 0, & 0, & \omega_2, & -\frac{i}{2}(\zeta_3 - \zeta_4), & \frac{i}{2}(\kappa_2 - \zeta_2), & \frac{1}{2}(\zeta_3 + \zeta_4), & \frac{1}{2}(\kappa_2 + \zeta_2) \\ \frac{1}{2}(\kappa_1 + \zeta_1), & \frac{1}{2}(\zeta_3 + \zeta_4), & -\frac{i}{2}(\kappa_1 - \zeta_1), & \frac{i}{2}(\zeta_3 - \zeta_4), & \omega_1, & 0, & 0, & 0 \\ \frac{1}{2}(\zeta_3 + \zeta_4), & \frac{1}{2}(\kappa_2 + \zeta_2), & \frac{i}{2}(\zeta_3 - \zeta_4), & -\frac{i}{2}(\kappa_2 - \zeta_2), & 0, & \omega_2, & 0, & 0 \\ \frac{i}{2}(\kappa_1 - \zeta_1), & -\frac{i}{2}(\zeta_3 - \zeta_4), & \frac{1}{2}(\kappa_1 + \zeta_1), & \frac{1}{2}(\zeta_3 + \zeta_4), & 0, & 0, & \omega_1, & 0 \\ -\frac{i}{2}(\zeta_3 - \zeta_4), & \frac{i}{2}(\kappa_2 - \zeta_2), & \frac{1}{2}(\zeta_3 + \zeta_4), & \frac{1}{2}(\kappa_2 + \zeta_2), & 0, & 0, & 0, & \omega_2 \end{bmatrix} \quad (\text{C.6})$$

References

- [1] R. N. Mohapatra, Phys. Rev. Lett. **56** (1986), 561-563. R. N. Mohapatra and J. W. F. Valle, Phys. Rev. D **34** (1986), 1642
- [2] A. Zee, Phys. Lett. **161B**, 141 (1985). E. Ma, Phys. Rev. Lett. **81**, 1171 (1998) [hep-ph/9805219]. T. P. Cheng and L. F. Li, Phys. Rev. D **22** (1980), 2860
- [3] A. Zee, Nucl. Phys. **B 264**, 99 (1986); K. S. Babu, Phys. Lett. B **203**, 132 (1988); M. Aoki, S. Kanemura, T. Shindou, and K. Yagyu, J. High Energy Phys. **10 1007** (2010) 084; J. High Energy Phys. **11** (2010) 049; G. Guo, X. G. He, and G. N. Li, J. High Energy Phys. **10** (2012) 044; Y. Kajiyama, H. Okada, and K. Yagyu, Nucl. Phys. **B874**, 198 (2013).
- [4] M. Aoki, S. Kanemura, and O. Seto, Phys. Rev. Lett. **102**, 051805 (2009); M. Aoki, S. Kanemura, and O. Seto, Phys. Rev. D **80**, 033007 (2009).
- [5] L. M. Krauss, S. Nasri, and M. Trodden, Phys. Rev. D **67**, 085002 (2003). A. Ahriche and S. Nasri, JCAP **07** (2013), 035 [arXiv:1304.2055 [hep-ph]]. A. Ahriche, K. L. McDonald and S. Nasri, Phys. Rev. D **92** (2015) no.9, 095020 [arXiv:1508.05881 [hep-ph]].
- [6] T. Nomura and H. Okada, Phys. Lett. B **755**, 306 (2016) [arXiv:1601.00386 [hep-ph]].
- [7] K. Cheung and O. Seto, Phys. Rev. D **69** (2004), 113009 [arXiv:hep-ph/0403003 [hep-ph]].
- [8] A. Ahriche, S. Nasri and R. Soualah, Phys. Rev. D **89** (2014) no.9, 095010 [arXiv:1403.5694 [hep-ph]]. C. Guella, D. Cherigui, A. Ahriche, S. Nasri and R. Soualah, Phys. Rev. D **93**, no. 9, 095022 (2016) [arXiv:1601.04342 [hep-ph]], D. Cherigui, C. Guella, A. Ahriche and S. Nasri, Phys. Lett. B **762**, 225 (2016) [arXiv:1605.03640 [hep-ph]],
- [9] Y. Cai, J. Herrero-Garcia, M. A. Schmidt, A. Vicente and R. R. Volkas, Front. in Phys. **5**, 63 (2017) [arXiv:1706.08524 [hep-ph]]. S. M. Boucenna, S. Morisi and J. W. F. Valle, Adv. High Energy Phys. **2014** (2014), 831598 [arXiv:1404.3751 [hep-ph]].
- [10] E. Ma, Phys. Rev. D **73** (2006), 077301 [arXiv:hep-ph/0601225 [hep-ph]].
- [11] A. Ahriche, A. Jueid and S. Nasri, Phys. Rev. D **97** (2018) no.9, 095012 [arXiv:1710.03824 [hep-ph]].
- [12] A. Ahriche, A. Arhrib, A. Jueid, S. Nasri and A. de La Puente, Phys. Rev. D **101** (2020) no.3, 035038 [arXiv:1811.00490 [hep-ph]].
- [13] A. Ahriche, A. Jueid and S. Nasri, Phys. Lett. B **814** (2021), 136077 [arXiv:2007.05845 [hep-ph]].
- [14] P. Escribano, M. Reig and A. Vicente, JHEP **07** (2020), 097 [arXiv:2004.05172 [hep-ph]].
- [15] A. Ahriche, K. L. McDonald and S. Nasri, JHEP **06** (2016), 182 [arXiv:1604.05569 [hep-ph]]. A. Beniwal, J. Herrero-García, N. Leerdam, M. White and A. G. Williams, JHEP **21** (2020), 136 [arXiv:2010.05937 [hep-ph]]. D. M. Barreiros, F. R. Joaquim, R. Srivastava and J. W. F. Valle, JHEP **04** (2021), 249 [arXiv:2012.05189 [hep-ph]]. Z. L. Han, R. Ding, S. J. Lin and B. Zhu, Eur. Phys. J. C **79** (2019) no.12, 1007 [arXiv:1908.07192 [hep-ph]]. C. H. Chen and T. Nomura, JHEP **10** (2019), 005 [arXiv:1906.10516 [hep-ph]]. Z. L. Han and W. Wang, Eur. Phys. J. C **79** (2019)

- no.6, 522 [arXiv:1901.07798 [hep-ph]]. W. Wang, R. Wang, Z. L. Han and J. Z. Han, Eur. Phys. J. C **77** (2017) no.12, 889 [arXiv:1705.00414 [hep-ph]]. D. M. Barreiros, H. B. Camara and F. R. Joaquim, [arXiv:2204.13605 [hep-ph]]. D. Hehn and A. Ibarra, Phys. Lett. B **718** (2013), 988-991 [arXiv:1208.3162 [hep-ph]]. G. Cacciapaglia and M. Rosenlyst, JHEP **09** (2021), 167 [arXiv:2010.01437 [hep-ph]].
- [16] J. Aalbers *et al.* [LUX-ZEPLIN], [arXiv:2207.03764 [hep-ex]].
- [17] B. Grzadkowski, O. M. Ogreid and P. Osland, Phys. Rev. D **80** (2009), 055013 [arXiv:0904.2173 [hep-ph]].
- [18] L. Sarma, P. Das and M. K. Das, Nucl. Phys. B **963** (2021), 115300 [arXiv:2004.13762 [hep-ph]]. L. Sarma, B. B. Boruah and M. K. Das, Eur. Phys. J. C **82** (2022) no.5, 488 [arXiv:2106.04124 [hep-ph]].
- [19] J. A. Casas and A. Ibarra, Nucl. Phys. B **618** (2001), 171-204 [arXiv:hep-ph/0103065 [hep-ph]].
- [20] A. G. Akeroyd, A. Arhrib and E. M. Naimi, Phys. Lett. B **490** (2000), 119-124 [arXiv:hep-ph/0006035 [hep-ph]].
- [21] K. Kannike, Eur. Phys. J. C **72** (2012), 2093 [arXiv:1205.3781 [hep-ph]].
K. Kannike, Eur. Phys. J. C **76** (2016) no.6, 324 [erratum: Eur. Phys. J. C **78** (2018) no.5, 355] [arXiv:1603.02680 [hep-ph]]. K. Kannike, Eur. Phys. J. C **81** (2021) no.10, 940 [arXiv:2109.01671 [hep-ph]]. A. Ahriche, G. Faisel, S. Y. Ho, S. Nasri and J. Tandean, Phys. Rev. D **92** (2015) no.3, 035020 [arXiv:1501.06605 [hep-ph]].
- [22] T. Toma and A. Vicente, JHEP **01** (2014), 160 [arXiv:1312.2840 [hep-ph]].
- [23] M. Chekkal, A. Ahriche, A. B. Hammou and S. Nasri, Phys. Rev. D **95**, no. 9, 095025 (2017). [arXiv:1702.04399 [hep-ph]].
- [24] J. Abdallah *et al.* [DELPHI], Eur. Phys. J. C **31** (2003), 421-479 [arXiv:hep-ex/0311019 [hep-ex]].
- [25] E. Lundstrom, M. Gustafsson and J. Edsjo, Phys. Rev. D **79** (2009), 035013 [arXiv:0810.3924 [hep-ph]].
- [26] W. Grimus, L. Lavoura, O. M. Ogreid and P. Osland, Nucl. Phys. B **801** (2008), 81-96 [arXiv:0802.4353 [hep-ph]].
- [27] [ATLAS], ATLAS-CONF-2017-047.
- [28] A. Djouadi, Phys. Rept. **457** (2008), 1-216 [arXiv:hep-ph/0503172 [hep-ph]].
- [29] [ATLAS], ATLAS-CONF-2018-031.
- [30] X. G. He, T. Li, X. Q. Li, J. Tandean and H. C. Tsai, Phys. Rev. D **79** (2009), 023521 [arXiv:0811.0658 [hep-ph]].
- [31] Y. Meng *et al.* [PandaX-4T], Phys. Rev. Lett. **127** (2021) no.26, 261802 [arXiv:2107.13438 [hep-ex]].
- [32] E. Aprile *et al.* [XENON], JCAP **04** (2016), 027 [arXiv:1512.07501 [physics.ins-det]].

- [33] J. Billard, L. Strigari and E. Figueroa-Feliciano, Phys. Rev. D **89** (2014) no.2, 023524 [arXiv:1307.5458 [hep-ph]].
- [34] F. Ambrogi, C. Arina, M. Backovic, J. Heisig, F. Maltoni, L. Mantani, O. Mattelaer and G. Mohlabeng, Phys. Dark Univ. **24** (2019), 100249 [arXiv:1804.00044 [hep-ph]].
- [35] A. Alloul, N. D. Christensen, C. Degrande, C. Duhr and B. Fuks, Comput. Phys. Commun. **185** (2014), 2250-2300 [arXiv:1310.1921 [hep-ph]].
- [36] <https://feynrules.irmp.ucl.ac.be/wiki/2IDM3N>
- [37] A. Ahriche, S. M. Boucenna and S. Nasri, Phys. Rev. D **93** (2016) no.7, 075036 [arXiv:1601.04336 [hep-ph]].
- [38] R.A. Horn and C.R. Johnson, "Topics in Matrix Analysis", Cambridge University Press 1994.
- [39] T. Takagi, Japan J. Math **1** (1925) 83.